Supplementary Information for:

Bimodal Accurate H_2O_2 Regulation to Equalize Tumor-Associated Macrophage Repolarization and Immunogenic Tumor Cell Death Elicitation

Yan Zhao[a], Weiheng Kong[a], Jianqing Zhu[c], Fengli Qu*[b]

[a] College of Chemistry and Chemical Engineering, Qufu Normal University, Qufu, Shandong 273165, China

[b] Zhejiang Cancer Hospital, Hangzhou Institute of Medicine, Chinese Academy of Sciences, Hangzhou, Zhejiang 310022, China

[c] Department of Gynecologic Oncology, University Cancer Hospital of Chinese Science Academy, Hangzhou, Zhejiang 310004, China

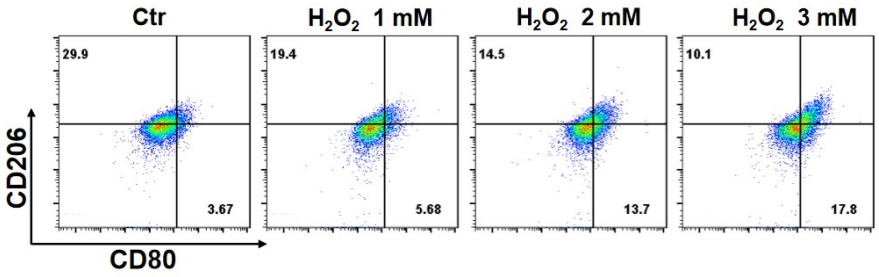

Figure S1. Population changes of RAW264.7 M1 ($CD80^{high}CD206^{low}$) macrophages after different concentrations of H_2O_2 incubation.

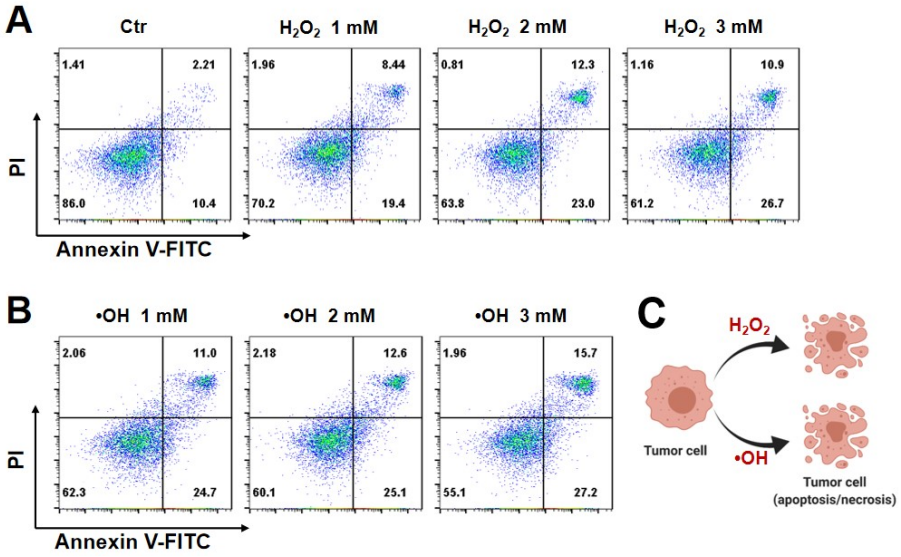

Figure S2. Apoptosis/necrosis of 4T1 cells treated with different concentrations of (a) H_2O_2 or (b) •OH. (c) Schematic diagram showing apoptosis/necrosis of 4T1 cells after different stimuli.

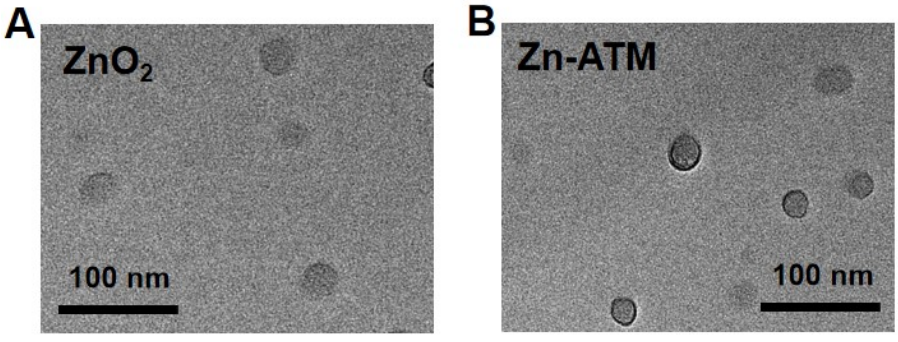

Figure S3. TEM images of (a) ZnO_2 and (b) Zn-ATM.

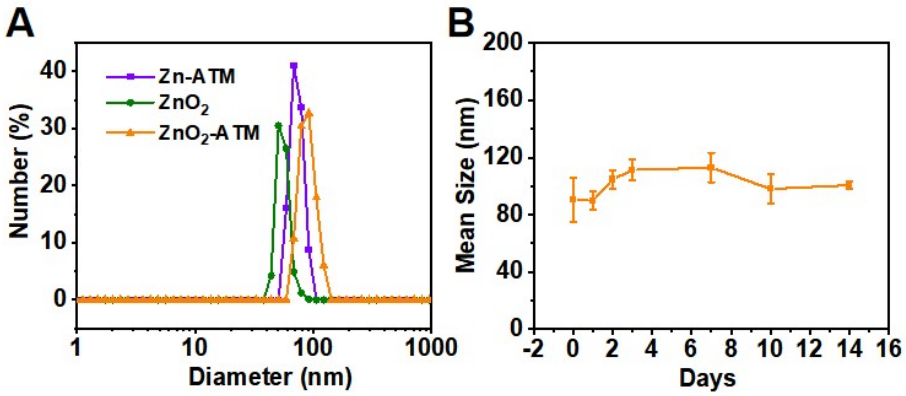

Figure S4. (a) DLS of corresponding nanoparticles dispersed in water. (b) DLS size of ZnO_2-ATM dispersed in water for various times.

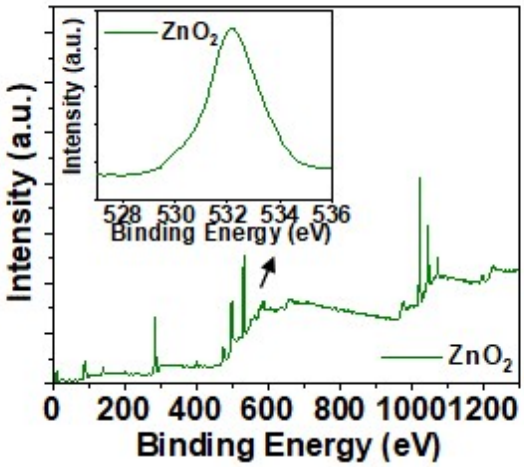

Figure S5. XPS survey spectrum of ZnO_2; inset shows O *1s* XPS spectrum of ZnO_2.

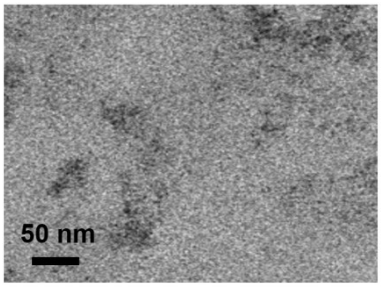

Figure S6. TEM image of ZnO_2-ATM after 24 h of incubation at pH 5.0.

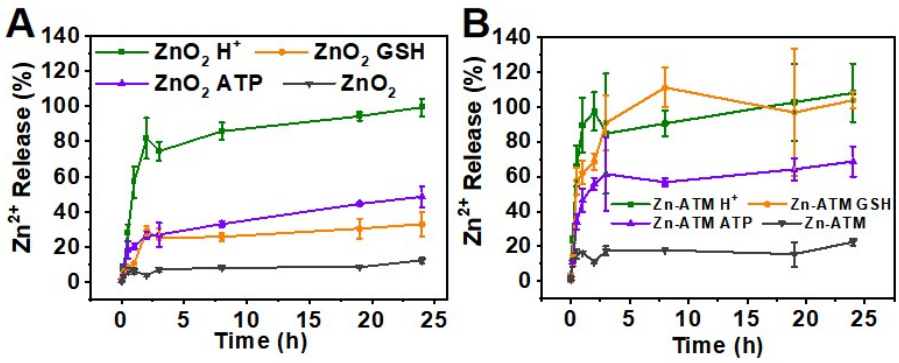

Figure S7. Zn^{2+} release from (a) ZnO_2 or (b) Zn-ATM after incubation with different solution conditions.

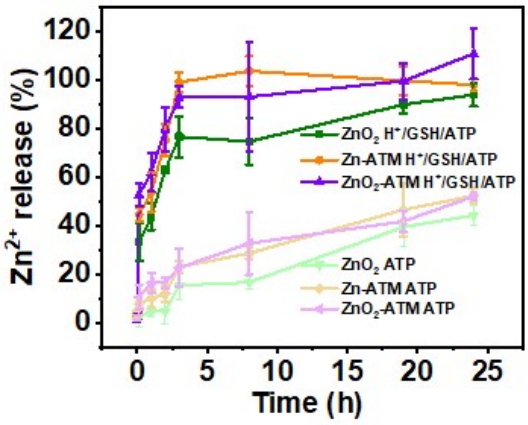

Figure S8. Zn^{2+} release from corresponding nanoparticles after incubation with the emulated tumor environment (pH = 5.0, GSH: 5 mM; ATP: 200 μg/mL) and the emulated immune environment (ATP: 200 μg/mL).

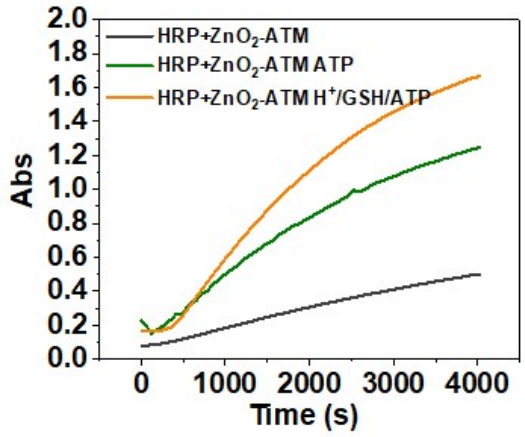

Figure S9. The kinetic spectroscopies of •OH generation of ZnO_2-ATM + HRP after incubation with the emulated tumor environment (pH = 5.0, GSH: 5 mM; ATP: 200 μg/mL) and the emulated immune environment (ATP: 200 μg/mL).

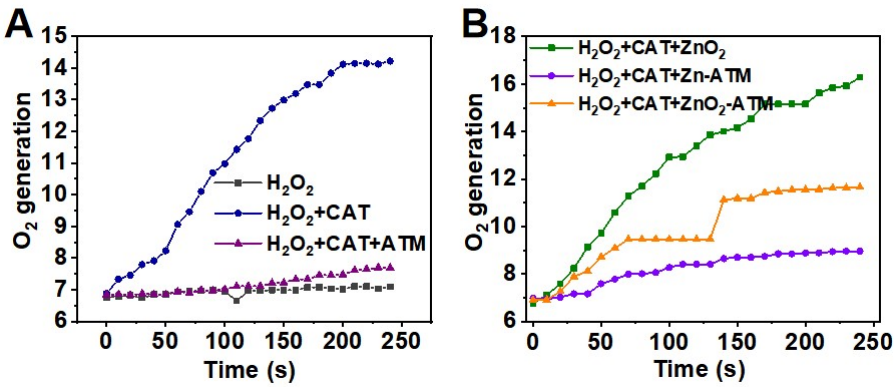

Figure S10. (a) O_2 generation of H_2O_2 + CAT in the presence of ATM or not. (b) O_2 generation of H_2O_2 + CAT in the presence of corresponding nanoparticles.

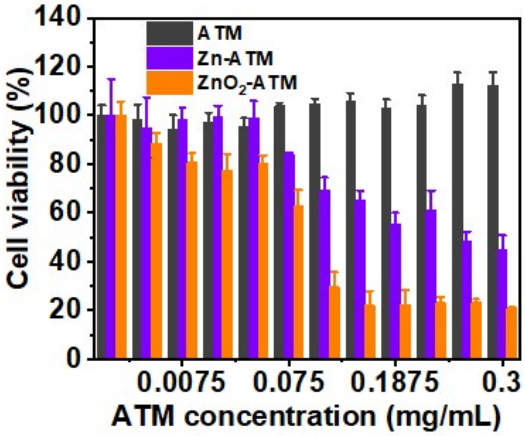

Figure S11. Cell viability of 4T1 cells incubated with different concentrations of corresponding nanoparticles (quantification by ATM).

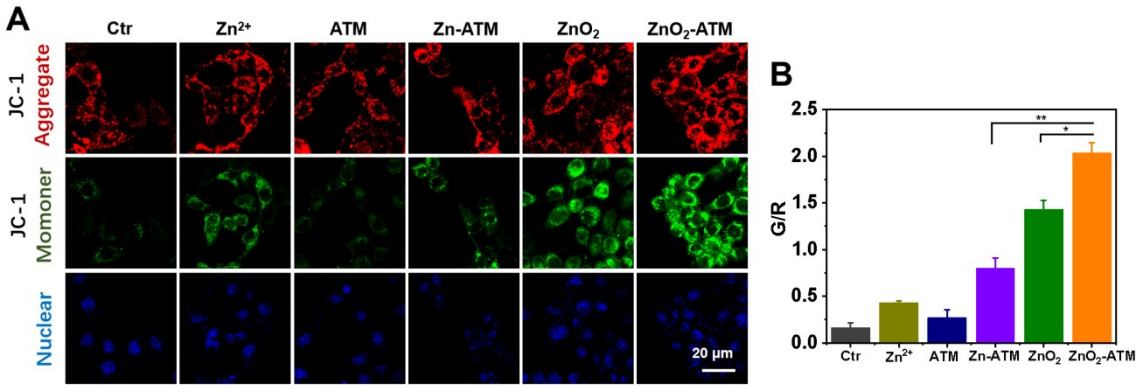

Figure S12. (a) Confocal images of JC-1 staining after various treatments (green: monomer; red: aggregates; blue: nuclear). (b) Quantification of Green/Red intensity after various treatments.

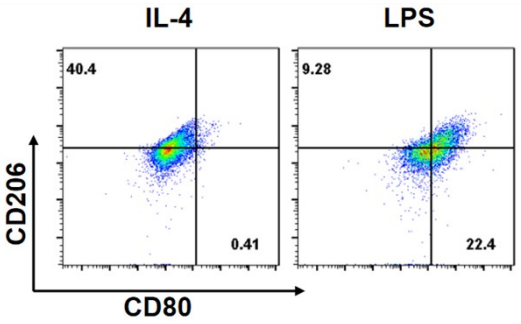

Figure S13. Population changes of M1 ($CD80^{high}CD206^{low}$) RAW264.7 macrophages after LPS or IL-4 incubation.

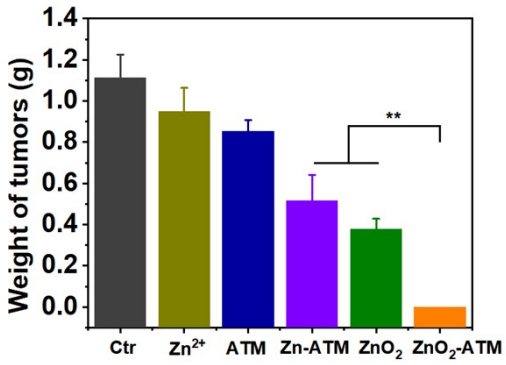

Figure S14. Average primary tumor weights from different treatment groups at 14 days post- injection.

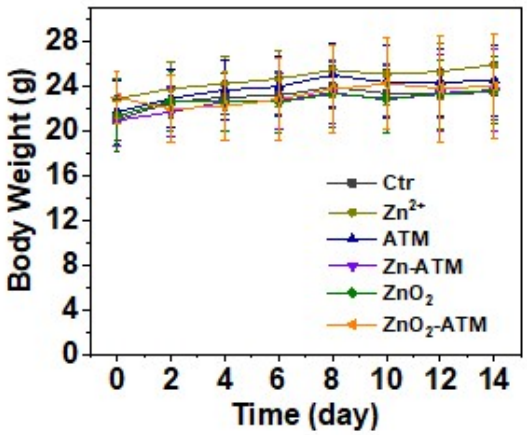

Figure S15. Average body weight curves of mice of different groups recorded after different treatments.

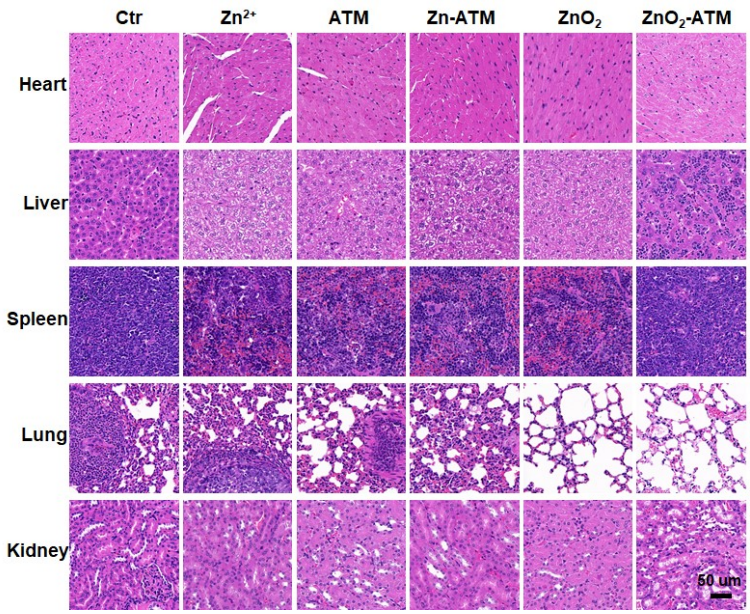

Figure S16. H&E-stained organ slices at 14 days post-injection of corresponding treatments.

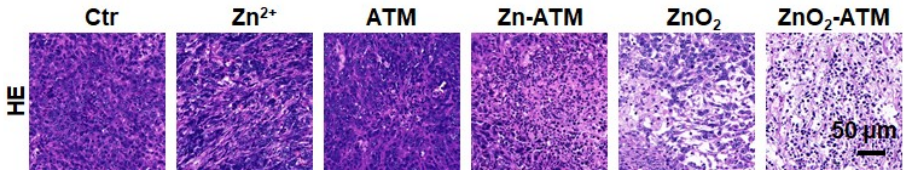

Figure S17. H&E-stained primary tumor slices at 1-day post-injection.

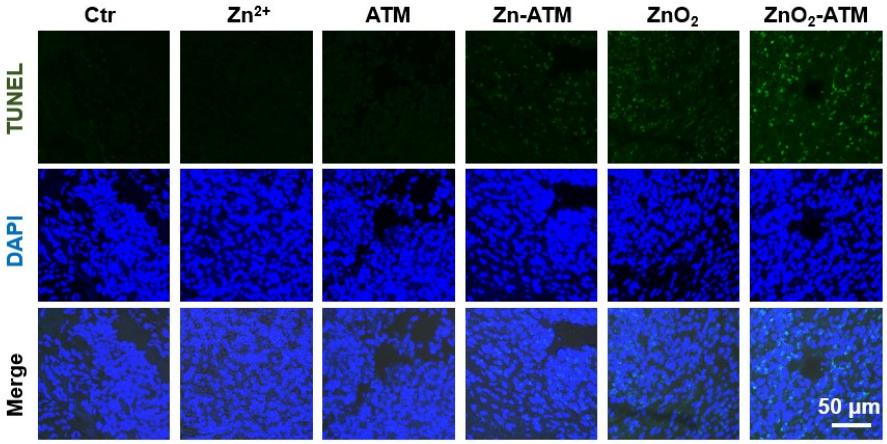

Figure S18 TUNEL immunofluorescence (blue: nucleus; green: apoptosis) of primary tumor slices at 1 day post-injection.

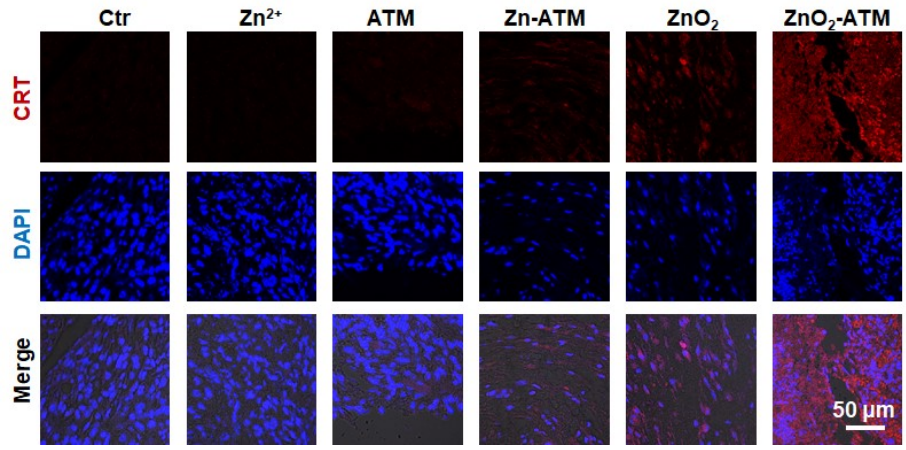

Figure S19. CRT immunofluorescence (blue: nucleus; red: CRT) of primary tumor slices at 1 day post-injection.

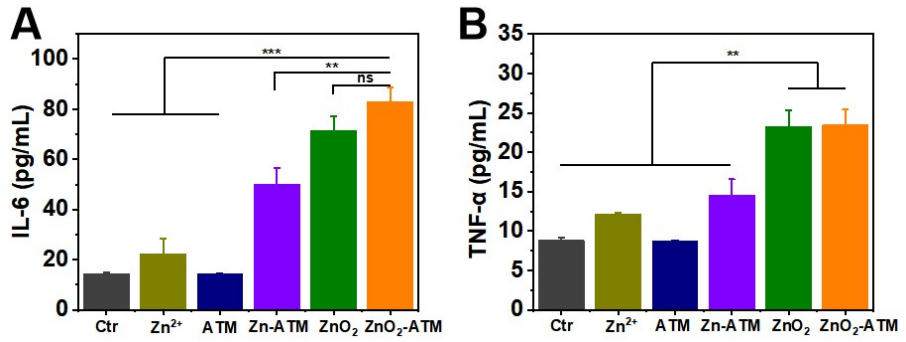

Figure S20. (a) IL-6 and (b) TNF-α of primary tumor at 3 days post-injection.

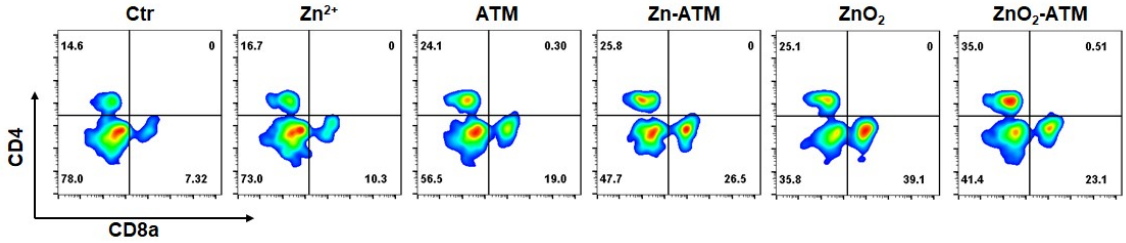

Figure S21. T-cell infiltration of primary tumors under different treatment groups at 3 days post- injection.

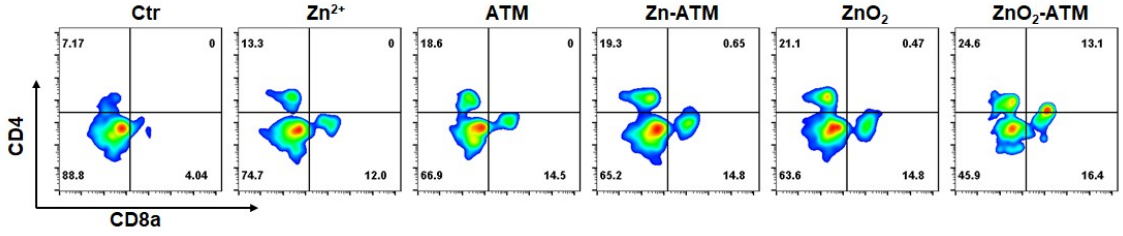

Figure S22. T-cell infiltration of distant tumors under different treatment groups at 14 days post- injection.

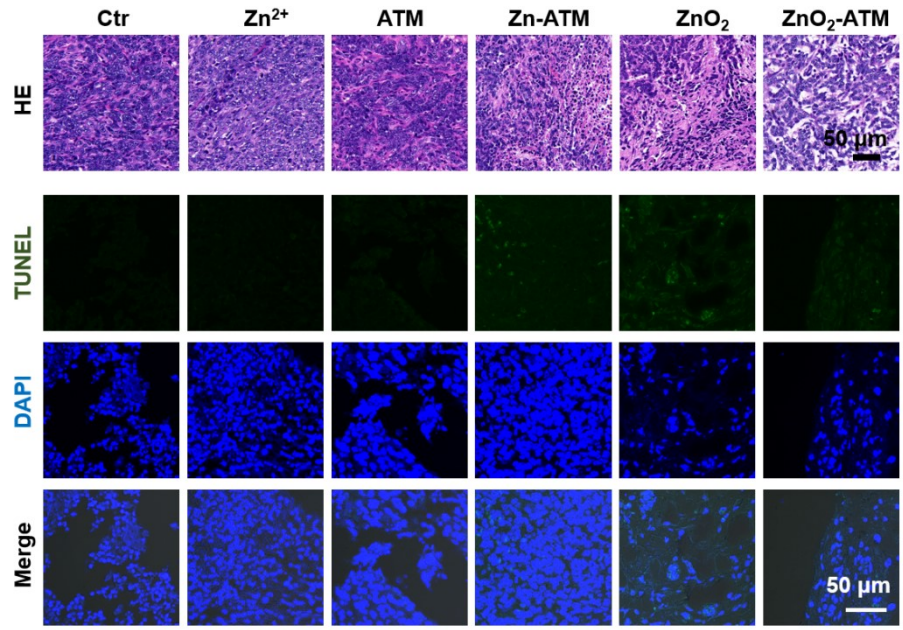

Figure S23. (a) H&E-stained distant tumor slices at 14 days post-injection. (b) TUNEL immuno-fluorescence (blue: nucleus; green: apoptosis) of distant tumor slices at 14 days post-injection.

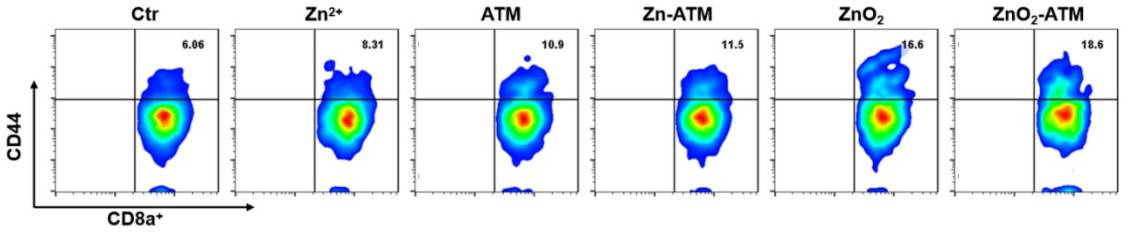

Figure S24. Memory T-cell production in the spleen under different treatment groups at 20 days post-injection.

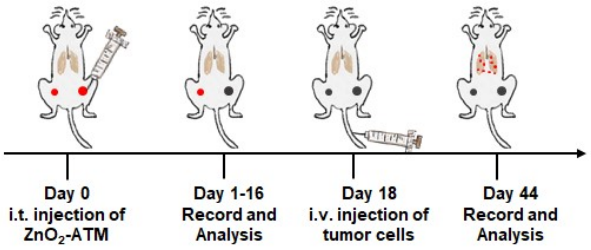

Figure S25. Lung metastasis model construction.

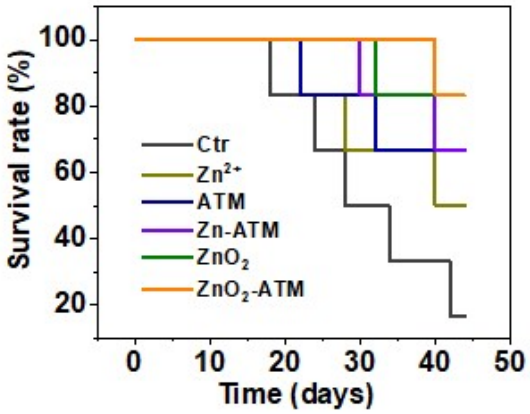

Figure S26. Survival rate of mice under different treatment groups.

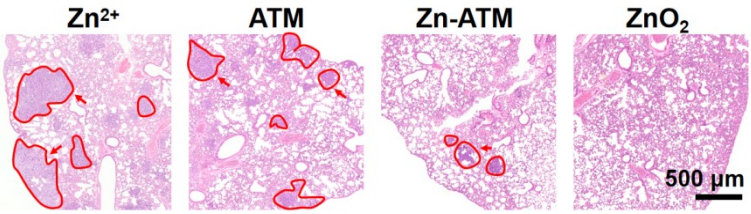

Figure S27. H&E-stained lung sections at 44 days post-injection. Red arrows indicate metastases.